Anisotropic Structure and Transformation Kinetics of Vapor-Deposited Indomethacin Glasses

Kevin J. Dawson,[†] Lei Zhu,[†] Lian Yu,[‡] and M. D. Ediger*,[†]

Department of Chemistry and School of Pharmacy, University of Wisconsin—Madison, Madison, Wisconsin 53706, United States

Received: September 28, 2010; Revised Manuscript Received: November 23, 2010

One- and two-dimensional wide-angle X-ray scattering (1D and 2D WAXS) measurements were performed on vapor-deposited glasses of indomethacin. Physical vapor deposition can be used to prepare organic glasses with high kinetic stability and other properties that are expected for glasses that have been aged for thousands of years. It was previously reported that 1D WAXS from such stable glasses contains an extra peak at $q = 0.6$ Å^{-1} that is not characteristic of the ordinary glass or expected for a highly aged glass. 2D WAXS measurements presented here show that the extra WAXS peak is caused by anisotropic packing in the vapor-deposited glass. The electron density is modulated normal to the film surface with a period roughly equal to the center of mass separation of indomethacin molecules. When such samples are annealed, the packing in the sample becomes isotropic. The transformation time for this process is much longer than the structural relaxation of the supercooled liquid and has a weaker temperature dependence. The observed temperature dependence of the transformation time is consistent with a growth front mechanism for the conversion of the stable glass into the supercooled liquid.

Introduction

A method has recently been discovered that allows the preparation of amorphous solids that have the properties expected for highly aged glasses.[1] These materials can be prepared by physical vapor deposition when the correct substrate temperature (T_{sub}) and deposition rate are used. These materials are called amorphous because, like liquid-cooled glasses, they have broad X-ray diffraction patterns.[2] As compared to ordinary glasses formed by cooling a supercooled liquid, these vapor-deposited materials show higher mobility onset temperatures,[3−6] larger enthalpy overshoots,[4−7] lower heat capacities,[8] lower water vapor uptake,[9] higher densities,[1,10,11] and higher moduli.[12] Because these new materials are stable to temperatures considerably higher than the conventional glass transition temperature T_g, they are often described as stable glasses. The vapor-deposited samples are so stable that it has been estimated that it would take over 1000 years of aging to produce samples with the same properties even though the vapor deposition process requires only a few hours.[7] Stable glasses have now been prepared from many different molecules[4] and could have technological utility as vapor deposition is used to make thin amorphous films for organic electronics.[13,14] It has been shown already that by simply changing the deposition temperature the lifetime of devices made by vapor deposition can be enhanced.[13] It is also possible that next-generation photolithography will employ vapor-deposited amorphous films.[15,16]

In addition to having properties that would be expected for highly aged glasses, stable vapor-deposited films have two properties that were not expected. The most stable vapor-deposited glasses of the glass-forming drug indomethacin[2] show a large extra peak in wide-angle X-ray scattering (WAXS) measurements; these samples were vapor-deposited at low rates onto substrates held near $0.84T_g$. Such a peak was not anticipated since WAXS measurements in the supercooled liquid above T_g show very little temperature dependence. In addition, aging an ordinary glass for more than a month did not produce any sign of an extra scattering peak. When the stable glass films were annealed above T_g, the extra WAXS peak slowly disappeared and the WAXS pattern of the supercooled liquid was recovered. Possible explanations[2] for the extra peak found in stable glasses include a first-order phase transition to a new packing arrangement below the conventional T_g and anisotropic packing.

The other unexpected property of stable vapor-deposited glasses is that thin films transform into the supercooled liquid via a surface-initiated growth front mechanism.[8,17−19] For ordinary glasses, a spatially homogeneous transformation from glass to supercooled liquid is observed when a sample is heated to near T_g.[20] It was shown by Kovacs that the time required for this transformation can be related to the structural relaxation time of the supercooled liquid as measured by dielectric spectroscopy or mechanical relaxation.[21,22] In contrast, for stable glass samples prepared at $0.84T_g$, a mobility front grows into the film at a constant velocity from the free surface (and sometimes from the glass/substrate interface).[17] The material behind the front is observed to mix like a supercooled liquid, while the material before the front remains in a vitrified state. However, the discovery of growth fronts in thin films does not explain how thick stable glass samples transform into the supercooled liquid. In contrast to thin films, the transformation time for thick films is independent of the sample dimensions.[8] Do thick stable glasses transform through a growth front mechanism or through a homogeneous transformation more similar to the behavior of ordinary glasses?

Here we use two-dimensional (2D) WAXS and one-dimensional (1D) WAXS to learn more about the unexpected scattering and transformation properties of stable indomethacin glasses. We used physical vapor deposition to prepare glass

* To whom correspondence should be addressed. E-mail: ediger@chem.wisc.edu.
[†] Department of Chemistry.
[‡] School of Pharmacy.

10.1021/jp1092916
Published on Web 12/17/2010

samples with a variety of substrate temperatures and deposition rates. The structures of the as-deposited samples were analyzed by 1D and 2D WAXS. We also measured the time required to transform as-deposited samples into the supercooled liquid during annealing with 1D WAXS and quasi-isothermal temperature-modulated differential scanning calorimetry (qi-TMDSC). Samples were annealed both in ambient relative humidity and under dry nitrogen.

We find that the extra WAXS peak of stable indomethacin glasses results from anisotropic packing. It originates from a modulation of electron density in the direction normal to the substrate surface with a period roughly equal to the spacing between molecules. Thus, the extra WAXS peak found in stable glasses is consistent with increased ordering along the direction of deposition. When the as-deposited samples are annealed isothermally in the vicinity of T_g, the anisotropic WAXS peak disappears as the sample transforms into an isotropic liquid. The temperature dependence of this process follows the temperature dependence of the growth front velocity. A correlation exists between the magnitude of the anisotropic WAXS feature and the kinetic stability of the vapor-deposited glasses. At substrate temperatures near $0.7T_g$, the anisotropic peak is no longer present, but other new features in the WAXS indicate changes in molecular packing.

Materials and Methods

Materials. Crystalline indomethacin (IMC, 1-(4-chlorobenzoyl)-5-methoxy-2-methyl-3-indoleacetic acid) with a purity of greater than 99% was obtained from Sigma and used without further purification. For the 2D WAXS experiments, samples were deposited onto Si[100] wafers (25.4 mm diameter, 250 μm thickness, single-side-polished) from Virginia Semiconductor. For 1D WAXS experiments, samples were vapor-deposited onto Si[510] wafers (24 mm diameter, 1 mm thick, single-side-polished) obtained from Gem Dugout (State Park, PA).

Methods. Physical vapor deposition was carried out in a manner similar to what has been previously described.[2,9,23] Inside the vacuum chamber, wafers or differential scanning calorimetry (DSC) pans were attached to a temperature-controlled stage using thermal contact grease. A crucible of IMC was heated to obtain the desired deposition rate as monitored by a quartz crystal microbalance. When the desired rate was achieved, the source was moved under the wafer/pans to start the deposition. The errors in the deposition conditions were ± 1 K for the substrate temperature and $\pm 15\%$ for the deposition rate. The samples were approximately 20 μm thick for WAXS measurements and approximately 40 μm thick for DSC. After the depositions were complete, the DSC pans were hermetically sealed. Both the DSC and WAXS samples were stored with desiccant in the freezer to prevent aging prior to measurements.

The 2D WAXS measurements were taken on a Bruker Hi-Star using Cu Kα ($\lambda = 1.54$ Å) X-rays in a reflection geometry. For most measurements, the sample plane and the X-ray beam made an angle of 4°, corresponding to near grazing incidence. A data collection time of 30 min was used for each frame. To compensate for defects in the frames caused by detector inhomogeneity, five successive frames were taken, with the detector being translated between each frame. The five frames were averaged using Datasqueeze taking into account the detector translation. Area integrations were performed using the GADDS controller software.

The 1D WAXS experiments were performed in a manner similar to what has been previously described.[2] A Bruker D8 Advance was used in a Bragg−Brentano configuration using Cu Kα X-rays. The samples were scanned from $q = 0.35$ Å^{-1} to $q = 2.45$ Å^{-1} with a step size 0.002 Å^{-1} and an integration time of 4 s per step. A 0.6 mm wide receiver slit was used which induced a broadening of ~0.002 Å^{-1}. A 21-point smooth (decreasing the resolution to 0.008 Å^{-1}) was applied to the raw data, after which a background scan was subtracted; no further corrections were applied to the data. Integrations of the 1D data were performed using Origin 8.

1D WAXS measurements were also performed to monitor structural changes occurring during isothermal annealing near T_g. Sample annealing was carried out in a custom-made oven either under ambient humidity or under a flow of dry nitrogen gas. Periodically, the samples would be removed from the oven for a WAXS scan at room temperature and ambient humidity and, after the measurement, returned to the oven. The "dry" samples were placed in a nitrogen environment for 5−16 h prior to further annealing to remove any water that may have been absorbed during the X-ray measurements; this time is sufficient to remove water from 20 μm stable glass samples.[9] WAXS measurements were repeated until the WAXS pattern of the ordinary glass was obtained for at least three consecutive annealing steps. The transformation time for the as-deposited sample to transform into the supercooled liquid was defined as the time at which ΔI decreased below a value of 0.05 (see eq 1).

The procedure utilized for the qi-TMDSC experiments has been previously reported.[23] A roughly 40 μm film of IMC was vapor-deposited into aluminum pans attached to the temperature-controlled stage. After the deposition, the pans were hermetically sealed using a DSC pan press. During this process, the samples were exposed to ambient relative humidity for 5−10 min. The pans were then stored in a desiccator in a freezer until testing. No attempt was made to remove any water that had absorbed into the films prior to sealing; previous experiments have shown that 10 min allows for an absorption of less than 0.1 wt % water at this thickness.[9] The qi-TMDSC measurements, performed with a TA Instruments Q2000 differential scanning calorimeter, utilized isothermal annealing at temperatures between 319 and 323 K ($T_g + 4$ K to $T_g + 8$ K). Throughout the measurement, a periodic temperature modulation was applied with a period of 60 s and a peak-to-peak amplitude of 0.5 K, allowing the reversible heat capacity, C_p, of the system to be measured as a function of the annealing time. The initial heating from room temperature to the annealing temperature required about 200 s. The starting time ($t = 0$) is defined by the first time that the sample reaches the annealing temperature. The annealing time required for the sample C_p to change 95% of the way from its initial value to the supercooled liquid C_p is defined as the transformation time for qi-TMDSC measurements.

Results

2D WAXS. Figure 1a shows the 2D WAXS pattern for a stable IMC glass sample. Two areas of high X-ray scattering intensity (yellow regions) are clearly observed. To aid in the interpretation of these data, two concentric circles have been added to the frame as dashed lines. The center of the circles marks $q = 0$, i.e., the position where the incident X-ray beam would have hit the detector had it not been blocked by the silicon substrate. The inner circle is placed at $q = 0.6$ Å^{-1} and the outer circle at $q = 1.4$ Å^{-1}. Normally X-ray scattering from a glass produces a radially symmetric pattern in 2D WAXS as a result of the isotropic nature of the glass.[24] Instead a "semicircle" is observed at $q = 1.4$ Å^{-1} for this sample deposited at $0.84T_g$ and 0.2 nm/s; the reflection geometry in our experiments causes

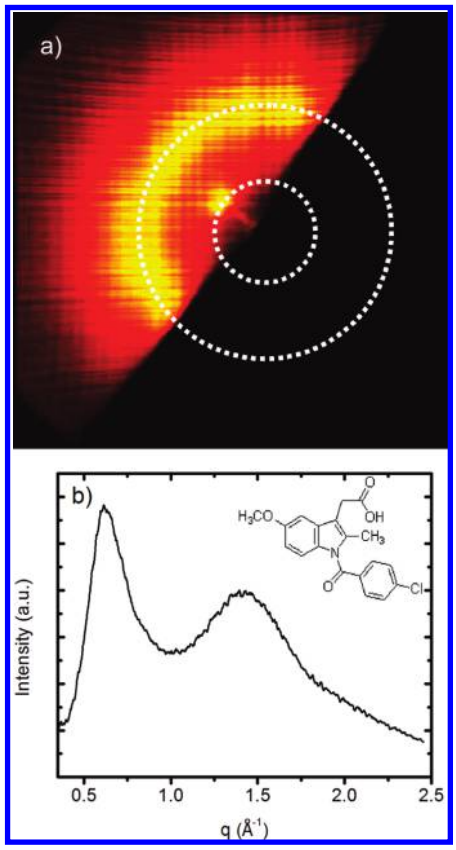

Figure 1. WAXS results for a stable glass of IMC. Panel a shows the 2D scattering pattern with two areas of high-intensity scattering. Panel b shows the 1D scattering curve, with peaks at 0.6 and 1.4 Å^{-1}; the circles in panel a are drawn at these two q values. In panel a, the scattering at 1.4 Å^{-1} is a segment of a circle as expected for an amorphous sample. In contrast, the scattering at 0.6 Å^{-1} is a spot that satisfies the Bragg condition and indicates that the electronic density varies periodically in the direction normal to the sample surface. This indicates that the sample is anisotropic. For both experiments, IMC samples were vapor-deposited at a rate of 0.2 nm/s onto substrates with $T_{sub} = 0.84T_g$. The molecular structure for IMC is shown as an inset in panel b.

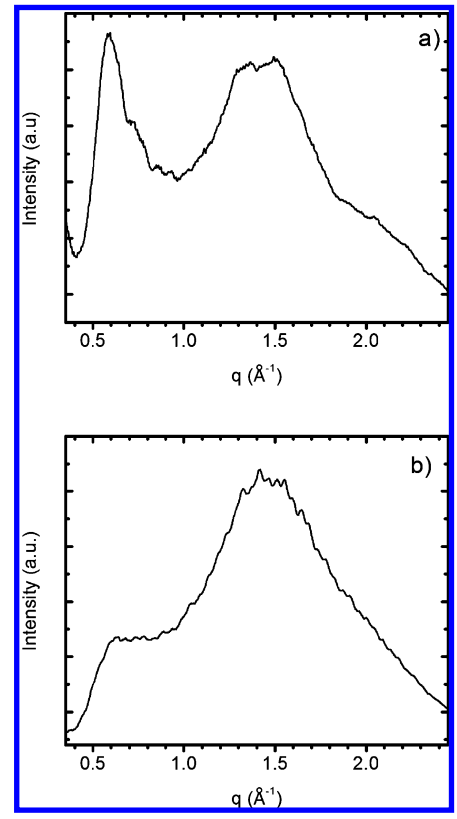

Figure 2. 1D powder patterns formed from the 2D WAXS measurement shown in Figure 1a. Panel a shows the result of integration across a small range of angles (10°) around the diffraction spot. Here two peaks are seen, similar to the 1D measurements on stable IMC glasses (Figure 1b). Panel b shows the result of integration over all the available data. In this case, only a peak and shoulder are observed. Thus, the peak at $q = 0.6$ Å^{-1} is indicative of in-plane, Bragg-like scattering.

the sample to block part of the detector and create a horizon. We expect that this higher q scattering would be radially symmetric if a transmission experiment could be performed on these samples. In contrast, the low q scattering in Figure 1a is clearly a spot, indicating that this scattering feature results from anisotropy in the sample.

Two additional experiments were performed to better understand the nature of the anisotropic scattering feature at $q = 0.6$ Å^{-1} in Figure 1a. A WAXS measurement was taken after the sample was rotated by 22° around the direction normal to the substrate surface (changing the ϕ angle). The resulting scattering pattern was identical to that shown in Figure 1a, suggesting that the spot is coming from in-plane scattering (Bragg-like diffraction). To test this interpretation, we measured the scattering at various X-ray incident angles from 1° to 6° using 1D WAXS and found that indeed the spot was the brightest when the Bragg condition was met, i.e., when the incident and scattering angles were equal (see Figure S1, Supporting Information).

It is important to establish the relationship between the 2D WAXS measurements reported here and the 1D WAXS measurements on stable IMC glasses that were reported previously.[2] One of those 1D measurements is reproduced in Figure 1b; the same deposition conditions were used to produce the samples in parts a and b of Figure 1. In qualitative agreement with Figure 1a, two peaks appear in the 1D scattering, at q values of 0.6 and 1.4 Å^{-1}. Furthermore, when the samples were annealed above T_g for several hours, the spot in Figure 1a disappeared in a manner consistent with the disappearance of the excess scattering at $q = 0.6$ Å^{-1} in the 1D WAXS measurements.[2]

To further illustrate the connection between 1D and 2D WAXS measurements, radial integrations of Figure 1a were performed, and these results are shown in Figure 2. Figure 2a roughly mimics the 1D WAXS experiments by integrating a "pie slice" of width 10° around the maximum of the peak at 0.6 Å^{-1}; in this integration, only data with the same absolute value of q are combined. For Figure 2b, all the data in the 2D WAXS pattern are integrated. Figure 2a reveals a pattern with two peaks that is very similar to what is observed for stable IMC glass in 1D WAXS (Figure 1b). In Figure 2b, the excess scattering at $q = 0.6$ Å^{-1} is almost negligible, indicating that the anisotropic scattering is a small fraction of the total WAXS intensity from these samples.

Influence of the Deposition Conditions on the Initial Structure (1D WAXS). Figure 3 compares 1D WAXS measurements from as-deposited IMC samples prepared on substrates with different temperatures. All the samples were prepared at a deposition rate of 0.2 nm/s. At the highest substrate temperature, the entire scattering curve is similar to what has been reported in the literature for the supercooled liquid and ordinary glass of IMC.[2,25] At high q values, the different substrate temperatures produce samples that are very similar in

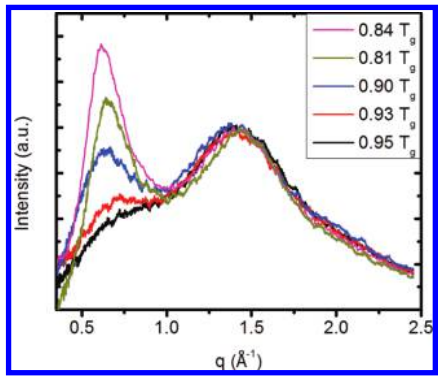

Figure 3. 1D WAXS measurements on IMC glasses deposited onto substrates at various temperatures. The largest amount of anisotropic scattering (peak at 0.6 Å^{-1}) is produced with T_{sub} near $0.84T_g$. All samples were prepared at a deposition rate of 0.2 nm/s.

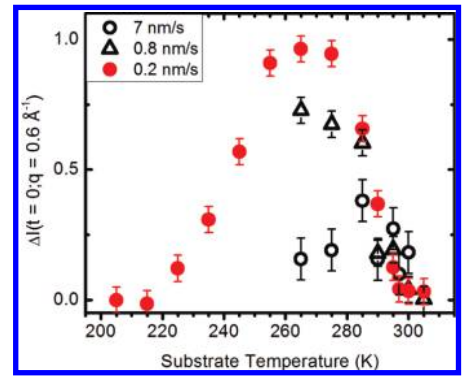

Figure 4. Magnitude of the anisotropic WAXS peak for IMC samples deposited at various substrate temperatures, for three different deposition rates. ΔI is defined in eq 1. For a deposition rate of 0.2 nm/s, a maximum is observed in ΔI at $0.84T_g$. The data points in this figure represent the average anisotropic magnitudes of all samples made at the given deposition conditions.

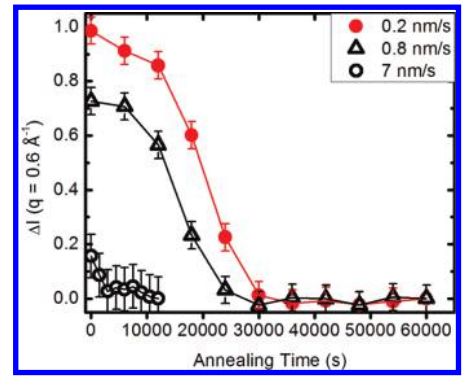

Figure 5. Time evolution of the anisotropic WAXS peak during annealing at 319 K (T_g + 4 K). These three samples were prepared at T_{sub} = 265 K at the deposition rates indicated and annealed under ambient relative humidity. For lower deposition rates, a larger initial anisotropic peak is observed and longer transformation times are required to obtain the supercooled liquid.

appearance with a peak at 1.4 Å^{-1}. In contrast, the scattering at low q depends strongly on the substrate temperature. As the substrate temperature is lowered, the anisotropic peak is observed to increase in intensity, reaching a maximum when $T_{sub} = 0.84T_g$, below which the intensity of the anisotropic peak decreases.

To investigate the important influence of deposition conditions on the size of the anisotropic peak, nearly 30 samples were prepared using various deposition rates and substrate temperatures. To compare these samples, we quantify the size of the anisotropic peak by integrating the scattering intensity over wave vectors near 0.6 Å^{-1}. This integration was carried out for each as-deposited sample, each sample after it had been annealed to the equilibrium supercooled liquid, and any annealing steps before equilibrium was attained. Equation 1

$$\Delta I(t;q{=}0.6\ \text{Å}^{-1}) = \frac{\int_{0.5}^{0.92} I(t;q)\,dq - \int_{0.5}^{0.92} I(t{=}\infty;q)\,dq}{\int_{0.5}^{0.92} I(t{=}\infty;q)\,dq} \quad (1)$$

defines ΔI as the excess scattering near 0.6 Å^{-1} relative to the scattering observed after the equilibrium supercooled liquid state has been reached. In eq 1, $I(t;q)$ is the intensity at an arbitrary annealing time t and $I(t{=}\infty;q)$ is the intensity after the sample has been annealed to equilibrium.

Figure 4 shows the average magnitude of the anisotropic scattering for IMC glass samples prepared at different deposition rates and substrate temperatures. At temperatures close to T_g (315 K) and at very low temperatures, little or no anisotropic scattering is observed. At intermediate substrate temperatures, the amount of anisotropic scattering depends upon the deposition rate. The most intense anisotropic scattering is observed at the lowest deposition rate with a substrate temperature of $0.84T_g$. These conditions also produce glasses with the highest density and the highest mobility onset temperature in a DSC experiment.[3,7,26] These connections will be discussed below.

Transformation into the Supercooled Liquid (1D WAXS). When as-deposited IMC glasses are heated above T_g, the peak at 0.6 Å^{-1} disappears over time as illustrated in Figure 5. This indicates a loss of anisotropy in the sample that we associate with the sample transforming into the equilibrium supercooled liquid. The three samples shown in Figure 5 were prepared with a substrate temperature of 265 K but with different deposition rates. They were annealed at 319 K in ambient relative humidity. As expected from Figure 4, more anisotropic scattering is initially observed from the sample with the lowest deposition rate. As can be seen in Figure 5, the time required to transform the samples into the supercooled liquid increases with decreasing deposition rate. This is consistent with DSC measurements on stable glasses where lower deposition rates lead to greater kinetic stability.[7,23] The decay curves in Figure 5 for the two lower deposition rates have similar shapes; we discuss this point below in relation to our proposed transformation mechanism. For further analysis, we define the transformation time as the first annealing point with a ΔI value of less than 0.05.

The transformation times for WAXS samples annealed in ambient relative humidity at 319 K are shown in Figure 6. The transformation times follow the same trends as the amplitude of the anisotropic scattering (Figure 4), except that the largest anisotropy occurs at T_{sub} = 265 K while the longest transformation time occurs at T_{sub} = 255 K. Some WAXS samples were omitted from Figure 6 because either the initial anisotropy in the sample was too small to accurately determine the transformation time or the transformation was completed during the first annealing step.

To complement the WAXS measurements, we measured the reversible heat capacity, C_p, of some stable glass samples during isothermal annealing with qi-TMDSC.[23] With time, C_p increases from the value of the as-deposited glass to that of the supercooled liquid. Hence, the time required to transform the stable glass into the supercooled liquid can be obtained. Figure

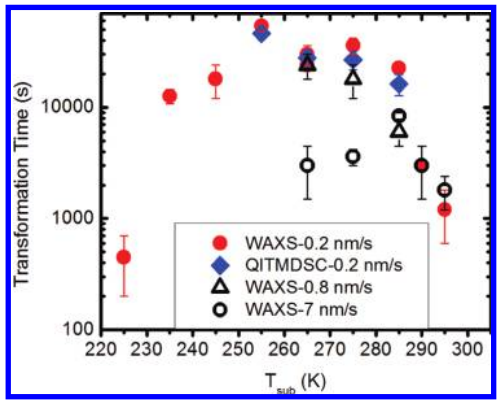

Figure 6. Transformation times for samples of IMC prepared at various substrate temperatures and deposition rates. All samples were annealed at 319 K, with the WAXS samples annealed under ambient relative humidity.

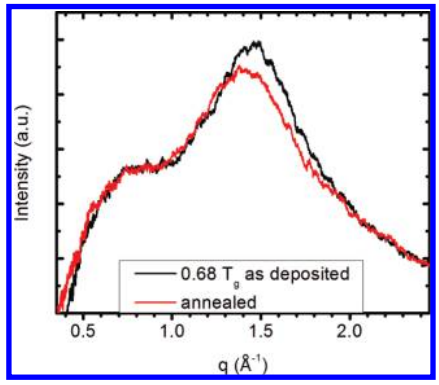

Figure 7. WAXS measurement for an IMC sample prepared at T_{sub} = 215 K and 0.2 nm/s, along with the measurement obtained after the sample was annealed at 319 K for 600 s. The as-deposited sample shows excess scattering near 1.4 Å^{-1} (not at 0.6 Å^{-1}). This type of excess scattering is a general feature for IMC samples prepared at substrate temperatures of less than 0.75T_g. The annealed sample attains the supercooled liquid packing in ≤600 s, indicating that the as-deposited glass is much less stable than samples prepared at 265 K.

6 shows the results of qi-TMDSC measurements performed on samples deposited at 0.2 nm/s and substrate temperatures ranging from 255 to 285 K.

Structure and Stability Resulting from Low-Temperature Deposition (1D WAXS). At low deposition temperatures, no anisotropic peak is seen in the WAXS at 0.6 Å^{-1}, but other changes indicate a different packing in the as-deposited sample as compared to the ordinary glass or equilibrium supercooled liquid. Figure 7 shows the WAXS pattern for a sample prepared at 0.2 nm/s and 215 K (0.68T_g). This deposition temperature is far below the substrate temperature that produces the maximum anisotropic scattering (0.84T_g). For samples deposited at 215 K, there is no anisotropic scattering at 0.6 Å^{-1} ($\Delta I = 0$) but the peak at 1.4 Å^{-1} does change with annealing. During annealing, this latter peak shifts to lower q by roughly 0.1 Å^{-1} and becomes slightly broader. Unlike the peak at 0.6 Å^{-1}, which for some samples can persist for over 20 000 s during annealing at 319 K, the sample prepared at 215 K annealed to equilibrium in less than 600 s. 2D WAXS experiments were also performed on a sample prepared at 215 K and 0.2 nm/s; the excess scattering near 1.4 Å^{-1} in this sample appears to be isotropic given our signal-to-noise ratio (data not shown). The low-temperature packing shown in Figure 7 is observed for substrate temperatures as high as 245 K but is not present at 255 K or above. The WAXS pattern for a sample deposited at 245 K is presented in the Supporting Information (Figure S2).

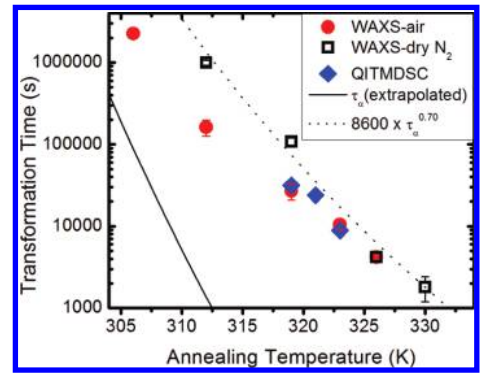

Figure 8. Effect of the annealing conditions on the transformation times for stable IMC glass. Data from both WAXS and qi-TMDSC are shown. All samples were prepared at 0.84T_g and a deposition rate of 0.2 nm/s. The solid line shows the α relaxation time of supercooled IMC extrapolated below the conventional T_g using the Vogel–Tammann–Fulcher (VTF) fit from the supercooled liquid (from ref 27). The dotted line shows the temperature dependence of the α relaxation time (measured and extrapolated portions) raised to a power of 0.7. The transformation times of the dry samples do not follow the temperature dependence of τ_α. Their weaker temperature dependence is consistent with transformation via growth fronts.

Influence of the Annealing Conditions on the Transformation Kinetics. Figure 8 shows the time required to transform stable IMC glasses into the supercooled liquid at different annealing temperatures and relative humidities. As expected for any activated process, the samples transform faster at higher temperatures. For comparison, the structural relaxation time, τ_α, of supercooled IMC (extrapolated from measurements of the super-cooled liquid above 315 K by dielectric relaxation[27]) is plotted as a solid line. It is clear that the transformation times substantially exceed τ_α and have a weaker temperature dependence.

The WAXS results in Figure 8 shows that stable IMC glasses transform considerably more slowly in a dry environment than at ambient relative humidity, particularly at lower annealing temperatures. It is known that ordinary IMC glass absorbs water and that this enhances molecular mobility.[28] We have previously shown that stable IMC glass absorbs about 5 times less water than ordinary IMC glass.[9] Nevertheless, Figure 8 shows that the limited water uptake of stable IMC glasses can decrease the transformation time near T_g by about a factor of 10. The merging of the data sets for dry and ambient relative humidity conditions at high temperature suggests that water uptake is less significant at higher temperature. For polymeric glasses it has been shown that vapor uptake does in fact decrease as the temperature increases.[29,30] We find it surprising that such a small amount of water uptake can change the mobility by the magnitude shown in Figure 8 and do not currently have a detailed explanation beyond the fact that water increases the mobility of IMC. As shown by the dotted line, the temperature dependence of the transformation time for dry stable glasses roughly tracks $\tau_\alpha^{0.70}$; the significance of this is discussed below.

Figure 8 also shows transformation times obtained for qi-TMDSC experiments at four annealing temperatures. Since these samples were annealed in sealed pans under a flow of nitrogen gas, we had expected that their transformation times would match those of the dry WAXS samples. The experiments at 319 K, however, indicate a better correspondence between the qi-TMDSC sample and the ambient relative humidity WAXS results. Even though the qi-TMDSC samples could absorb at

most 0.1 wt % water prior to sealing, apparently this is enough to significantly alter the transformation time.

Discussion

We have shown that vapor deposition can produce IMC glasses with wide-angle X-ray scattering significantly different from that of the ordinary glass or the equilibrium supercooled liquid. At substrate temperatures above 225 K, a new peak is observed at low q that results from anisotropic packing. When this peak is larger, the samples exhibit remarkable kinetic stability, resisting structural change for thousands of τ_α when heated above the conventional T_g. In this section we discuss the molecular origin of the anisotropic WAXS peak, the dependence of the peak size on the deposition conditions, and the kinetics of the transformation of bulk stable glasses.

Origin of the Anisotropic WAXS Peak at Low *q*. This work shows that the low-q peak observed for some vapor-deposited IMC glasses is caused by anisotropic packing. As illustrated in Figures 1 and 2, the extra peak mainly comes from in-plane scattering and appears only when we are close to the Bragg condition. Since the diffraction spot does not move when the sample is rotated, we conclude that the modulation of the electron density responsible for the new feature occurs primarily normal to the sample surface (z direction). The position of the peak at 0.6 $Å^{-1}$ indicates that the electron density has a real space periodicity of roughly 1 nm. Since this is approximately the center of mass spacing for IMC molecules, we conclude that the electron density modulation is caused by increased regularity of molecular packing along z. The observed scattering is consistent with an amorphous material with slightly increased long-range order and is possibly associated with some degree of molecular layering. If the sample were polycrystalline or crystalline, we would not expect to observe the broad amorphous halo at $q = 1.4$ $Å^{-1}$. The data are also inconsistent with a physical mixture of amorphous and polycrystalline phases.

It has been previously reported that physical vapor deposition can produce anisotropic amorphous materials. Reports of optical,[14,31−33] magnetic,[34−36] and even structural[37−41] anisotropy have been made over the past 20 years. Much of this work has been done on Fe/Tb glasses that exhibit magnetic anisotropy.[34,35,37−40,42,43] Deposition conditions can be found that cause Fe−Fe and Tb−Tb contacts to occur preferentially in the xy plane while Tb−Fe contacts occur predominantly in the z direction.[37,42] Hellman has explained much of the available data with a model based on surface ordering. At high temperatures, enough mobility exists at the deposition surface to allow adatom clusters to align, minimizing the surface energy.

Optical anisotropy has recently been reported in vapor-deposited organic systems containing a single component. Yokoyama et al. reported that vapor deposition of rodlike or planar molecules produced amorphous films with optical birefringence.[14,31,32] The difference in index of refraction values ($n_{xy} - n_z$) ranged from 0.04 for the smaller molecules to 0.25 for larger molecules.[31] They also reported a deposition temperature dependence for the measured properties for 4,4′-bis[(*N*-carbazole)styryl]biphenyl (BSB-Cz); depositions at $0.93T_g$ produced more optically isotropic films than depositions at $0.77T_g$.[14] This behavior may be related to the strong temperature dependence of anisotropic packing in IMC films, as shown in Figure 4.

X-ray scattering experiments were also carried out by Yokoyama et al. on the BSB-Cz films deposited at different substrate temperatures.[14] In contrast to our results, Yokoyama did not observe the emergence of an extra in-plane WAXS peak as the deposition temperature was lowered even though the optical anisotropy increased significantly. On the basis of optical absorption, Yokoyama concluded that the molecules in the film were packing such that the transition dipole moments were mostly parallel to the substrate surface.[14,31] Yokoyama hypothesized that the rodlike nature of the larger molecules caused them to flatten out onto the substrate during deposition, causing the transition dipole moments to predominately lie in the xy plane. To our knowledge, the work described here on IMC is the first report of a single-component molecular glass former with ordering in the z direction. Given that IMC is more nearly spherical than the molecules studied by Yokoyama, it is surprising that vapor deposition of IMC gives rise to an anisotropic WAXS peak since this was not observed for the systems studied by Yokoyama. The polar and hydrogen-bond-forming structure of the IMC molecule might be preferentially aligned in the polar environment of the surface during deposition.

Singh and de Pablo recently reported that stable glasses of trehalose could be prepared in a molecular dynamics simulation.[44] Interestingly, these simulated materials exhibit significant packing anisotropy and evidence of a layered structure that is qualitatively consistent with the WAXS data presented here. Simulations on systems for which WAXS and birefringence data exist may provide the best method for understanding the packing of stable glasses on a molecular level.

It might be thought that stable glasses are actually nanocrystalline and that the extra WAXS peak might somehow give evidence of this. As we have discussed previously,[2] we find this unlikely. Figure 8 shows that the anisotropic WAXS peak can be annealed away at temperatures as low as 306 K. If this is interpreted as the melting of nanocrystals, the Gibbs−Thomson equation can account for this melting point decrease (more than 100 K) only if the nanocrystals are 1−2 nm in size;[2] this would correspond to only 1 or 2 molecular diameters per crystal. To our knowledge, the nanocrystal hypothesis cannot account for the growth fronts observed in submicrometer films,[18] while in retrospect growth fronts can be rationalized for highly stable glasses.[1,8,12,45] Furthermore, while nucleation rates vary tremendously among organic liquids and glasses, the phenomenology of stable glass formation seems rather consistent for the roughly 10 systems studied thus far,[4] arguing that "stable glass" is a more accurate description of these results than "nanocrystalline". Thus, we interpret the WAXS measurements in Figure 1 as indicating amorphous packing that is mildly perturbed from the isotropic packing expected for supercooled liquids and ordinary glasses.

In a previous paper, we argued that the simplest explanation for the sudden appearance of the excess scattering as the deposition temperature is decreased is that IMC undergoes a polyamorphic transition below the conventional T_g.[2] In light of the 2D WAXS experiments reported here, our view has changed. At present, the simplest explanation for the excess scattering is that vapor deposition creates a glass that is mildly anisotropic but otherwise has local packing very similar to that of the ordinary supercooled liquid or glass. However, it is possible that stable IMC glasses are associated with a second local packing arrangement[23] and that more sophisticated structural measurements would indicate this.

Magnitude of the Anisotropic Packing Peak. Figure 4 shows that substrate temperatures near $0.84T_g$ produce vapor-deposited IMC glasses in which the anisotropic packing measured by WAXS is maximized. Lower deposition rates maximize the anisotropy, and this apparently contradicts the simplest explanation of stable glass formation. We have

previously explained the formation of stable glasses as a surface equilibration process.[1] If the surface of the glass has enhanced mobility, molecules arriving from the vapor phase can make use of this mobility to partially equilibrate at the substrate temperature. A recent simulation by Léonard and Harrowell illustrates that enhanced surface mobility can account for many of the features of stable glasses.[46] Up to the present, we have assumed that the most favorable local packing near the surface closely resembles packing in the bulk equilibrium supercooled liquid at the substrate temperature. This view successfully explains the higher density and lower enthalpy of glasses vapor-deposited at $0.84T_g$.[7,26] However, as the equilibrium supercooled liquid at $0.84T_g$ is assumed to be isotropic, it is challenging to explain how lower deposition rates (and the corresponding longer equilibration times) can lead to more anisotropic packing.

We tentatively explain the behavior shown in Figure 4 by proposing a mechanism that includes some molecular ordering at the glass/vapor interface. When the substrate temperature is $0.84T_g$, the layer of enhanced mobility is quite thin. Neutron reflectivity experiments on trinaphthylbenzene indicate a mobile layer of about one monolayer at this temperature.[1] Under these conditions, configurational sampling at the surface may lead to formation of anisotropic structures. This might happen because equilibration (at least on the time scale relevant to the experiment) is occurring in an almost 2D liquid. Under these circumstances, the packing between pairs of molecules might be similar to packing in the equilibrium supercooled liquid at $0.84T_g$, but the orientation of pairs of molecules (relative to the surface) might be systematically perturbed. Alternately, molecules directly at the surface might have a preferred orientation relative to the surface. It has been shown that molecules can align at a liquid surface even at temperatures above the bulk melting point, leading to the phenomenon of surface freezing.[47,48]

No matter what source might give rise to some preferred orientation in the very top layer during vapor deposition, once these molecules are buried by additional molecules arriving from the vapor phase, there may not be sufficient mobility to rearrange into the isotropic packing that is presumably favored by thermodynamics at the substrate temperature. It is perfectly reasonable that the hypothesized surface orientation would take some time to develop, and this would account for the observation in Figure 4 that slower deposition at $0.84T_g$ gives rise to more anisotropic packing. As discussed above, surface-induced anisotropy has previously been used by Hellman to explain the anisotropy observed in vapor-deposited Tb/Fe films.[49]

The mechanism described above can also account for the features of Figure 4 at higher substrate temperatures. At temperatures near T_g, the thickness of the mobile surface layer has been estimated to be about five monolayers.[26] Even if the top monolayer has some preferred orientation, enough mobility persists in the immediately adjacent layers to equilibrate to an isotropic liquid before further deposition kinetically locks the configuration. In this explanation, the crossover in the effect of the deposition rate that occurs near 292 K (Figure 4) indicates the temperature where the thickness of the mobile surface layer approaches one monolayer.

At very low substrate temperatures, Figure 4 shows that vapor-deposited samples do not show any evidence of molecular layering. At such low temperatures, surface mobility is presumably so small that there is no opportunity to organize into molecular layers at any accessible deposition rate. Under these conditions, the sample packing will be far from equilibrium (and may be anisotropic in other respects). The literature supports this idea with examples of vapor-deposited films produced below $0.75T_g$ that have higher enthalpy, lower density, or different packing compared with glasses produced by cooling from the supercooled liquid.[11,50−52]

Previous WAXS experiments by Ishii provide insight into the molecular packing that results from low-temperature depositions.[53,54] For vapor-deposited chlorobenzene and benzene, they report a broad amorphous peak at $q \approx 1.4$ Å^{-1}. This peak shifted slightly to higher q as the deposition temperature was lowered. They explained this change as a shift toward more random (less optimized) packing at lower temperatures. Ishii's results and explanation seem broadly consistent with the data in Figure 7. For IMC, the shift in peak position is accompanied by a dramatic loss of kinetic stability, as evidenced by the short time required to attain equilibrium packing during annealing.

Kinetics of Transformation into the Supercooled Liquid. In this section, we shift our perspective regarding the anisotropic WAXS peak found in some vapor-deposited IMC glasses. Rather than focus on its origin, we use its disappearance during annealing to assess kinetic stability. We associate the time required for the anisotropic peak to disappear with the transformation to the supercooled liquid. Substantial molecular motion is required to eliminate an electronic density modulation on the 1 nm length scale, and since this mobility is absent in the glass, it is reasonable to associate this motion with the appearance of the supercooled liquid. As shown in Figure 8, the time required for the anisotropic peak to disappear correlates well with the transformation into the supercooled liquid as determined from the heat capacity (qi-TMDSC).

One of the most striking features of Figure 8 is that the transformation time for a stable IMC glass can be much longer than the structural relaxation time, τ_α, of the supercooled liquid. At 312 K, transformation requires $10^3\tau_\alpha$, while $10^4\tau_\alpha$ is required at 330 K. For comparison, when an ordinary IMC glass is aged for more than a month at $T_g - 20$ K, transformation into the supercooled liquid requires less than $50\tau_\alpha$.[23] The high kinetic stability of these vapor-deposited glasses is in agreement with the view that stable glasses behave like highly aged ordinary glasses.[1]

An unusual feature of Figure 8 is the weak temperature dependence of the transformation times in comparison with τ_α. The experiments of Kovacs and Ferry are relevant here as a comparison.[21,22] They prepared a polymer glass and then measured volume relaxation during annealing at a series of temperatures near T_g. The equilibration time in these experiments matched the temperature dependence of τ_α as obtained from dielectric and mechanical experiments. In this respect, stable IMC glasses have a behavior different from what would be expected for a highly aged glass; i.e., the transformation time scales as $\tau_\alpha^{0.7}$ rather than as τ_α.

The relatively weak temperature dependence of the transformation times in Figure 8 raises the possibility of a distinct transformation mechanism for stable glasses as compared to ordinary glasses. It has already been reported that submicrometer films of stable IMC glass do not transform into the supercooled liquid homogeneously when heated. Instead, the liquid is observed to grow from the free surface of the material and propagate through the glass with a constant velocity.[18] The material before the front remains in an immobile glassy state, while the material behind the front is allowed to mix and diffuse like a supercooled liquid. These features of thin stable glasses have also been observed in a simulation of the deposition process that utilizes a kinetic Ising model.[46] It has also been reported that the transformation time for stable IMC glasses becomes independent of the film thickness above 1 μm.[8,19] Since the films

used for the WAXS and qi-TMDSC experiments are at least 20 μm thick, the transformation mechanism for thick films cannot be surface-initiated.

It was previously proposed that thick stable glass films might transform into the supercooled liquid via the nucleation and growth of supercooled liquid "bubbles" inside the stable glass.[8,26] In this scenario, nucleation sites would be separated by about 1 μm and the growth would occur at the same velocity as observed near the free surface.[8] We can test this view by comparing the temperature dependence shown in Figure 8 (for the dry samples) with that observed for growth fronts in thin films of IMC stable glasses. From nanocalorimetry the growth front velocity for IMC was found to change from 0.01 to 0.04 nm/s as the temperature was raised from 316 to 320 K.[8] This is consistent with a temperature dependence of $\tau_\alpha^{0.6}$, in reasonably good agreement with the dotted line in Figure 8.

The proposal that bulk stable glasses transform via multiple initiation sites coupled with constant velocity growth can be tested by fitting our WAXS data to an Avrami function. The Avrami function is commonly used in crystallization studies to deduce nucleation and growth parameters from measurements of the total crystallization as a function of time.[55,56] When fit to our data, the Avrami exponent is near 4; this is consistent with the idea of random nucleation of the supercooled liquid coupled with constant-velocity growth into the stable glass.[57] A table of fit parameters can be found in the Supporting Information.

There is theoretical work to support our hypothesis that thick stable glasses transform via the growth of liquid bubbles. Wolynes has proposed that aged glasses transform into the supercooled liquid beginning at "rejuvenation" centers in the glass.[45] The rest of the glass then transforms by fronts that spherically propagate from these nucleation points at a velocity related to the liquid mobility behind the front. If we accept that stable glasses behave like highly aged glasses, the Wolynes work can be directly applied to our experiments to explain why the transformation time is found to scale approximately as $\tau_\alpha^{0.70}$ in Figure 8. Near T_g, self-diffusion in supercooled liquids has a weaker temperature dependence than τ_α.[20,58] For IMC, Swallen et al.[59] report that self-diffusion in the supercooled liquid scales as $\tau_\alpha^{-0.77}$ in the temperature range of Figure 8.

Finally, we wish to consider the correlation between the magnitude of the anisotropic WAXS peak and the kinetic stability of stable glasses of IMC. Figure 6 shows that the time required to transform the samples from the as-deposited state into the supercooled liquid depends upon both the deposition temperature and the deposition rate. Similar dependences are observed for the magnitude of the anisotropic peak. In Figure 9 the unaveraged data points from Figures 4 and 6 are graphed against each other. A reasonably strong correlation is seen between ΔI and the time required to transform the sample at 319 K in ambient relative humidity.

The correlation shown in Figure 9 is reasonable given the mechanism discussed above, in that the conditions that produce the largest anisotropy peaks also produce glasses with the highest kinetic stability. At higher substrate temperatures, the deposited molecules cannot explore configurations that are drastically lower in energy than the ordinary glass, resulting in samples that have mild kinetic stability. At substrate temperatures far below $0.84T_g$, the molecules do not have the mobility to explore configurations that lead to kinetic stability. Between these two temperature regimes, the molecules have enough mobility to explore low-energy configurations and are thus kinetically stable. At these intermediate temperatures, the mobile layer is sufficiently thin that surface orientation effects cannot be relaxed

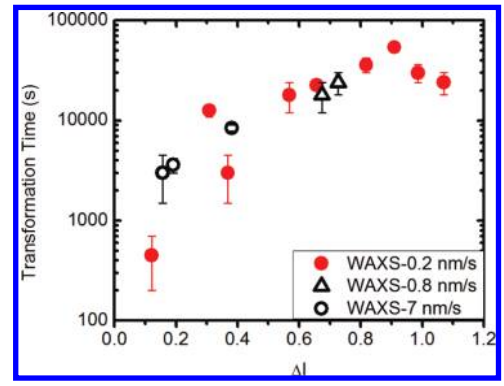

Figure 9. Correlation between the size of the anisotropic peak (ΔI) and the transformation time. While a correlation between the two properties is observed, the samples with the most anisotropic scattering do not have the longest transformation time. The data points shown here correspond to samples annealed under ambient relative humidity.

before configurations are trapped, and thus, an anisotropic material results. We speculate that if we were able to utilize much lower deposition rates, the correlation seen in Figure 9 would not hold. In this scenario, we imagine that deposition at $0.84T_g$ would produce samples with even more kinetic stability but with less anisotropy, because sufficient time would be provided for some equilibration of molecules not directly at the surface. There is some indication in Figure 9 that the most stable samples are not the most anisotropic. Perhaps this feature is related to our speculative comments above.

Concluding Remarks

Physical vapor deposition has been used to prepare glassy films of indomethacin using a variety of substrate temperatures and deposition rates. The films were analyzed by both 1D and 2D wide-angle X-ray scattering. We found that the extra WAXS peak found at low q in stable IMC glasses is a result of anisotropic packing in the film. The electron density is modulated in the direction normal to the film surface. At deposition temperatures lower than $0.84T_g$, the anisotropic peak is less prominent; in this regime, the WAXS measurements provide evidence of a different type of nonequilibrium packing.

The time required to anneal away the anisotropic peak can be much longer than the structural relaxation time, τ_α, of the supercooled liquid. For the most stable glasses, this transformation time has a weaker temperature dependence than does τ_α. This result is consistent with the proposal that bulk samples of stable glass transform into the supercooled liquid via growth fronts that initiate inside the film and then expand.

In this paper we do not directly address the question of how much anisotropic order is present at a molecular level in stable IMC glasses. We do not know, for example, whether one particular molecular axis is more likely to be found in the xy plane than in the z direction. We also do not know to what extent an isotropic packing arrangement needs to be perturbed to produce a low-q peak with the magnitude of those observed here. Such molecular information about stable glass packing is relevant for understanding to what extent the stable glasses investigated here can be regarded as models for the equilibrium supercooled liquid far below the conventional T_g. We are optimistic that these WAXS measurements, in combination with molecular simulations[44] and other techniques such as ellipsometry, can provide a more molecular view of the packing in stable glasses.

Anisotropic packing in organic materials may be technologically relevant. Yokoyama et al. have compared charge mobility

in organic glasses with different packing arrangements.[14] They reported that anisotropic packing can improve charge mobility by roughly an order of magnitude, presumably by optimizing the overlap between the π orbital systems of adjacent molecules. It is likely that a thorough understanding of physical vapor deposition will lead to the ability to produce multiple types of anisotropic packing arrangements and hence the ability to optimize packing for particular applications.

Acknowledgment. We thank the Department of Energy (Grant DE-SC0002161) and the National Science Foundation (Grant DMR 0804786) for supporting this research. We thank Don Savage, Mike Efremov, and Christoph Schick for useful discussions. We acknowledge the Materials Science Center at the University of Wisconsin—Madison for the use of their 2D WAXS instrument.

Supporting Information Available: Three figures and a table of additional information. This material is available free of charge via the Internet at http://pubs.acs.org.

References and Notes

(1) Swallen, S. F.; Kearns, K. L.; Mapes, M. K.; Kim, Y. S.; McMahon, R. J.; Ediger, M. D.; Wu, T.; Yu, L.; Satija, S. *Science* **2007**, *315*, 353.
(2) Dawson, K. J.; Kearns, K. L.; Yu, L.; Steffen, W.; Ediger, M. D. *Proc. Natl. Acad. Sci. U.S.A.* **2009**, *106*, 15165.
(3) Kearns, K. L.; Swallen, S. F.; Ediger, M. D.; Wu, T.; Yu, L. *J. Chem. Phys.* **2007**, *127*, 154702.
(4) Zhu, L.; Yu, L. *Chem. Phys. Lett.* **2010**, *499*, 62.
(5) Leon-Gutierrez, E.; Garcia, G.; Clavaguera-Mora, M. T.; Rodriguez-Viejo, J. *Thermochim. Acta* **2009**, *492*, 51.
(6) Leon-Gutierrez, E.; Garcia, G.; Lopeandia, A. F.; Clavaguera-Mora, M. T.; Rodriguez-Viejo, J. *J. Phys. Chem. Lett.* **2010**, *1*, 341.
(7) Kearns, K. L.; Swallen, S. F.; Ediger, M. D.; Wu, T.; Sun, Y.; Yu, L. *J. Phys. Chem. B* **2008**, *112*, 4934.
(8) Kearns, K. L.; Ediger, M. D.; Huth, H.; Schick, C. *J. Phys. Chem. Lett.* **2010**, *1*, 388.
(9) Dawson, K. J.; Kearns, K. L.; Ediger, M. D.; Sacchetti, M. J.; Zografi, G. *J. Phys. Chem. B* **2009**, *113*, 2422.
(10) Ishii, K.; Nakayama, H.; Hirabayashi, S.; Moriyama, R. *Chem. Phys. Lett.* **2008**, *459*, 109.
(11) Ishii, K.; Nakayama, H.; Moriyama, R.; Yokoyama, Y. *Bull. Chem. Soc. Jpn.* **2009**, *82*, 1240.
(12) Kearns, K. L.; Still, T.; Fytas, G.; Ediger, M. D. *Adv. Mater.* **2010**, *22*, 39.
(13) Kwong, C. Y.; Djurisic, A. B.; Roy, V. L.; Lai, P.; Chan, W. K. *Thin Solid Films* **2004**, *458*, 281.
(14) Yokoyama, D.; Setoguchi, Y.; Sakaguchi, A.; Suzuki, M.; Adachi, C. *Adv. Funct. Mater.* **2010**, *20*, 386.
(15) Pfeiffer, F.; Felix, N. M.; Neuber, C.; Ober, C. K.; Schmidt, H. W. *Adv. Funct. Mater.* **2007**, *17*, 2336.
(16) Pfeiffer, F.; Felix, N. M.; Neuber, C.; Ober, C. K.; Schmidt, H. W. *Phys. Chem. Chem. Phys.* **2008**, *10*, 1257.
(17) Swallen, S. F.; Traynor, K.; McMahon, R. J.; Ediger, M. D.; Mates, T. E. *Phys. Rev. Lett.* **2009**, *102*, 065503.
(18) Swallen, S. F.; Traynor, K.; McMahon, R. J.; Ediger, M. D.; Mates, T. E. *J. Phys. Chem. B* **2010**, *114*, 2635.
(19) Kearns, K. L.; Whitaker, K. R.; Ediger, M. D.; Huth, H.; Schick, C. *J. Chem. Phys.* **2010**, *133*, 014702.
(20) Swallen, S. F.; Traynor, K.; McMahon, R. J.; Ediger, M. D.; Mates, T. E. *J. Phys. Chem. B* **2009**, *113*, 4600.
(21) Kovacs, A. J.; Stratton, R. A.; Ferry, J. D. *J. Phys. Chem.* **1963**, *67*, 152.
(22) Kovacs, A. J. *J. Polym. Sci.* **1958**, *30*, 131.
(23) Kearns, K. L.; Swallen, S. F.; Ediger, M. D.; Sun, Y.; Yu, L. *J. Phys. Chem. B* **2009**, *113*, 1579.
(24) Alexander, L. E. *X-ray Diffraction Methods in Polymer Science*; John Wiley & Sons Inc.: New York, 1969.
(25) Bates, S.; Zografi, G.; Engers, D.; Morris, K.; Crowley, K.; Newman, A. *Pharm. Res.* **2006**, *23*, 2333.
(26) Swallen, S. F.; Kearns, K. L.; Satija, S.; Traynor, K.; McMahon, R. J.; Ediger, M. D. *J. Chem. Phys.* **2008**, *128*, 214514.
(27) Carpentier, L.; Decressain, R.; Desprez, S.; Descamps, M. *J. Phys. Chem. B* **2006**, *110*, 457.
(28) Andronis, V.; Zografi, G. *Pharm. Res.* **1998**, *15*, 835.
(29) Chang, M. J.; Myerson, A. S.; Kwei, T. K. *J. Appl. Polym. Sci.* **1997**, *66*, 279.
(30) Vitoux, P.; Tassaing, T.; Cansell, F.; Marre, S.; Aymonier, C. *J. Phys. Chem. B* **2009**, *113*, 897.
(31) Yokoyama, D.; Sakaguchi, A.; Suzuki, M.; Adachi, C. *Org. Electron.* **2009**, *10*, 127.
(32) Yokoyama, D.; Sakaguchi, A.; Suzuki, M.; Adachi, C. *Appl. Phys. Lett.* **2008**, *93*, 173302.
(33) Lin, H. W.; Lin, C. L.; Chang, H. H.; Lin, Y. T.; Wu, C. C.; Chen, Y. M.; Chen, R. T.; Chien, Y. Y.; Wong, K. T. *J. Appl. Phys.* **2004**, *95*, 881.
(34) Hellman, F.; Gyorgy, E. M. *Phys. Rev. Lett.* **1992**, *68*, 1391.
(35) Hellman, F.; Messer, M.; Abarra, E. N. *J. Appl. Phys.* **1999**, *86*, 1047.
(36) Chaudhar, P.; Cuomo, J. J.; Gambino, R. J. *Appl. Phys. Lett.* **1973**, *22*, 337.
(37) Harris, V. G.; Hellman, F.; Elam, W. T.; Koon, N. C. *J. Appl. Phys.* **1993**, *73*, 5785.
(38) Yan, X.; Hirscher, M.; Egami, T.; Marinero, E. E. *Phys. Rev. B* **1991**, *43*, 9300.
(39) Rhyne, J. J.; Pickart, S. J.; Alperin, H. A. *Phys. Rev. Lett.* **1972**, *29*, 1562.
(40) Hufnagel, T. C.; Brennan, S.; Zschack, P.; Clemens, B. M. *Phys. Rev. B* **1996**, *53*, 12024.
(41) Afanas'ev, V. V.; Stesmans, A.; Andersson, M. O. *Phys. Rev. B* **1996**, *54*, 10820.
(42) Harris, V. G.; Aylesworth, K. D.; Das, B. N.; Elam, W. T.; Koon, N. C. *Phys. Rev. Lett.* **1992**, *69*, 1939.
(43) Hufnagel, T. C.; Hellman, F. *J. Magn. Magn. Mater.* **2003**, *256*, 322.
(44) Singh, S.; De Pablo, J. J. *Proc. Natl. Acad. Sci. U.S.A.*, submitted for publication.
(45) Wolynes, P. G. *Proc. Natl. Acad. Sci. U.S.A.* **2009**, *106*, 1353.
(46) Léonard, S.; Harrowell, P. *J. Chem. Phys.*, in press, available at arXiv:1008.4438v1.
(47) Kawamata, M.; Yamamoto, T. *J. Phys. Soc. Jpn.* **1997**, *66*, 2350.
(48) Li, H. Z.; Yamamoto, T. *J. Chem. Phys.* **2001**, *114*, 5774.
(49) Hellman, F. *Appl. Phys. Lett.* **1994**, *64*, 1947.
(50) Ishii, K.; Nakayama, H.; Okamura, T.; Yamamoto, M.; Hosokawa, T. *J. Phys. Chem. B* **2003**, *107*, 876.
(51) Ishii, K.; Nakayama, H. *J. Non-Cryst. Solids* **2007**, *353*, 1279.
(52) Takeda, K.; Yamamuro, O.; Oguni, M.; Suga, H. *Thermochim. Acta* **1995**, *253*, 201.
(53) Ishii, K.; Yoshida, M.; Suzuki, K.; Sakurai, H.; Shimayama, T.; Nakayama, H. *Bull. Chem. Soc. Jpn.* **2001**, *74*, 435.
(54) Ishii, K.; Nakayama, H.; Yoshida, T.; Usui, H.; Koyama, K. *Bull. Chem. Soc. Jpn.* **1996**, *69*, 2831.
(55) Avrami, M. *J. Chem. Phys.* **1939**, *7*, 1103.
(56) Avrami, M. *J. Chem. Phys.* **1940**, *8*, 212.
(57) Hiemenz, P. C.; Lodge, T. P. *Polymer Chemistry*, 2nd ed.; CRC Press, Taylor & Francis Group: Boca Raton, FL, 2007.
(58) Mapes, M. K.; Swallen, S. F.; Kearns, K. L.; Ediger, M. D. *J. Chem. Phys.* **2006**, *124*, 054710.
(59) Swallen, S. F.; Ediger, M. D. Manuscript in preparation.

JP1092916